Design of a Remote Person View System for a Long Range UAV

Pedro Gersão Miller
pedrogmiller@gmail.com

Instituto Superior Técnico, Lisboa, Portugal

June 2015

Abstract

A solution for a remote person view using commercial off-the-shelf equipment is presented and analysed. For the success of this work, mission objectives and requirements were defined and explained, and an Unmanned Air System (UAS) design was proposed and evaluated through, not only, controlled environment but also flight testing. The performance of this UAS was, then, used to evaluate the choices made and purpose a definite and better solution for long range. The platform is composed by three main systems: the radio control, the video feed and the telemetry radio that together connect the air vehicle to the ground station. Although the long range system encountered difficulties in reaching a maximum flight range, it proved to be useful for long range applications.
Keywords: Video, Radio-Control, RPV, UAS, long range.

1. Introduction

Unmanned Aerial Systems (UASs) are remotely piloted systems (namely, a UAV and a ground station) which can be used for many applications where it may be inconvenient, dangerous or expensive to make use of manned flights. Their areas of application vary from search and rescue operations, fire-fighting, law enforcement, military and news reporting. Generally, the vehicle will have sensors to observe its environment and can autonomously make decisions about its behaviour or pass the information onto a human operator at a different location for control purposes.

Primarily, UAS serve as information gathering platforms. When compared to manned aircraft, they result in a decrease in the need for human operators and, consequently, lowers costs and risk. Additionally, because surveillance often requires flights of long durations, fatigue may limit the ability of human beings to maintain a high level of vigilance. They also offer advantages for information acquisitions where ground-based access is deemed too hazardous (in case of a crisis or disaster).
The objective of this work is to design and construct a platform system for remote-person view for the long endurance unmanned aerial vehicle (LEEUAV) that is being developed [1]. The expected results include detailed design, setup and testing of the control and video sub-systems for the UAS. The tests will be done in a way that both video and remote control are approved in a controlled environment and then perform a series of flight tests where both systems are evaluated in its range and quality. For the success of the flight tests there will also have to be telemetry data guidance from the UAV to the ground station.

2. Background

UASs have experienced a rapid development in its recent past. Some years back, only a restrict group of people knew what a UAV was, but now they seem to be everywhere. What happened is a classical case of an enabling technology being driven by the consumer market. Quilter and Anderson [2], mounted a 33 mm camera in a model airplane to obtain low altitude/large scale photography to document stream and riparian restoration projects.

The platform used by Hardin and Jackson [3], was designed to include remotely controlled airplane with a stabiliser, a 35 mm camera and a GPS receiver, Upon landing, the GPS data was downloaded to yield the plane vertical and horizontal positions and velocity. The photograph locations were found by following the GPS tracks.

In [4], a modified RC airplane equipped with a GPS receiver and a digital camera was proposed to conjunction with automated post-processing techniques to reduce the costs of traditional noxious weed mapping. The study found that automated post-processed photos were not positioned sufficiently accurate to produce consistent and accurate weed perimeters.

In 2012, Roberto Montiel broke the world record for range in a remote control model glider using a camera onboard. Most of the flight was done soaring power off, taking advantage of thermal air updrafts. The starting point was Algora, Spain and the route extended SouthEast 111 km and return to start, 222 km. The total flight time was 6 hours [5].

The glider used for this dissertation will be controlled using the long range radio communication system (LRS) as done in some of the works cited. Also, it is made use of a wireless security video system and a micro-controller to provide imagery and telemetry data to fly the UAS out of sight.

3. Methodology

3.1. Design Specification

The design was carried out with the specifications from Table 3.1.

Maximum Thrust	14 N.
Max. Payload:	1 kg
Max. Weight w/o payload:	1.6 kg
Total weight:	2.6 kg
Type of cells	3S LiPo
Estimate flight time - minutes	30
Range of radio frequency coverage	3-5 km
Range of video frequency coverage	6-7 km
Frequency of control signals	433 MHz
Frequency of video Transmission	1.2 GHz

3.2. Flight Controller Unit

The UAV is able to navigate autonomously by using a GPS receiver together with a compass sensor to detect accurately the UAV position in space, its height above sea level and its distance from a target location. This is done by implementing a GPS waypoint navigation algorithm that receives as input the UAV location and compass bearing signals and then directs the UAV to the desired location. The APM ardupilot is the chosen flight controller. It is a small computer running on an 8-bit AT Mega 1280 system at a frequency of 16 MHz with an 8 KB RAM. The block in Fig. 1 shows the input/output relationship of all other components to the flight controller [6].

3.3. Communications System

The remote controller Graupner mc-24 was selected as the primary input device to interact with the UAV. This remote controller is useful due to the many open channels available that enable a more complex configuration then the usual 4 channels (throttle, aileron, horizontal stabiliser and rudder) one.

A useful upgrade for this particular RC system is the Thomas Scherrer long range system (TSLRS) which is a RC control system designed for long

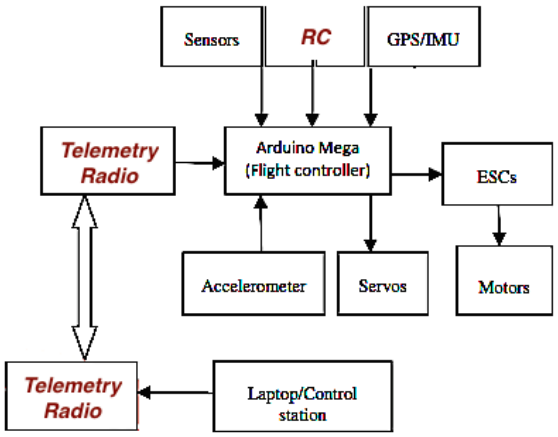

Figure 1: Block diagram showing the input/output relationship of other components to the flight controller.

range model planes. The receiver (Rx) transmits at a 433 MHz frequency, weighs 8 g, has an optimised input filter so it can co-exist with FPV transmitters and possesses a diversity system that is choosing the best receiving antenna from having two connected (this removes blind spots if one antenna is placed horizontally and the second is placed vertically). It operates through a UHF band (433 MHz to 440 MHz), has three output levels possible, 0.5, 1 and 2 W and has a Receiver Signal Strength Indication (RSSI) analogue output pin that proves to be extremely useful to check during flight [7].

This LRS with a monopole antenna on the ground station is advertised as having a range of 3 to 5 km with 500 mW in a normal city area. However, it is possible to get a much higher range by using an appropriate antenna configuration. On the UAV the standard wire antennas were chosen for its omni-directionality. On the ground station,was selected a Yagi-Uda antenna from DiammondAntennas (A430S10) with a gain of 13 dBi and 30° of beam width [8].

A block diagram of the entire RC unit is presented in Fig. 2.

3.4. Video System

The image capture device is a kx-181 Sony camera with 50 mAh consumption and weighs 26 g. It is connected to a 1.2 GHz transmitter with an output power of 850 mW which transmits wireless to a 1.2 GHz receiver and then to a DVR SD card recorder and a 10” display monitor [9].

The RPV system was designed to perform long range flights. Therefore, the antennas were properly selected. An omnidirectional Skew planar wheel antenna with circular polarization [10] for the UAV and a Helical antenna with 11 dBi for the ground station were selected. This combination is adver-

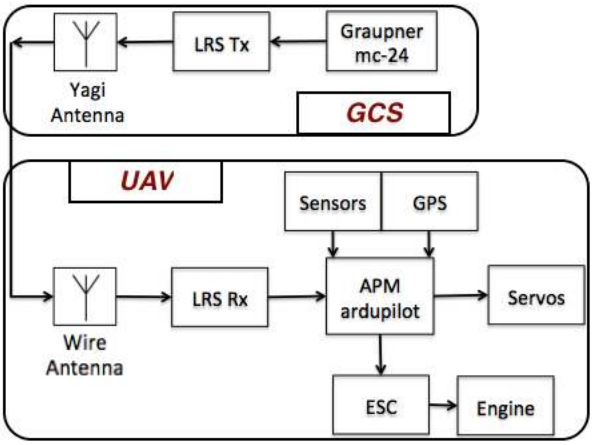

Figure 2: Block diagram showing the radio control (RC) sub-system.

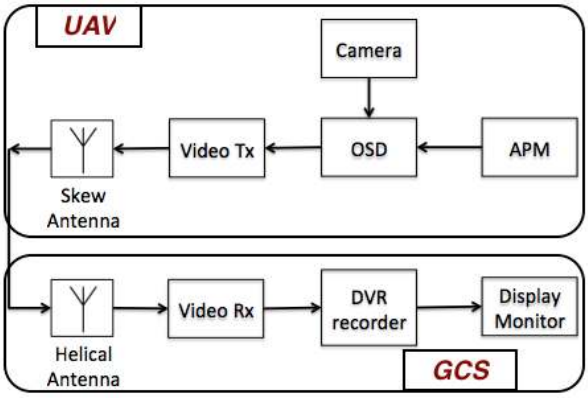

Figure 3: Block diagram showing the remote person view sub-system.

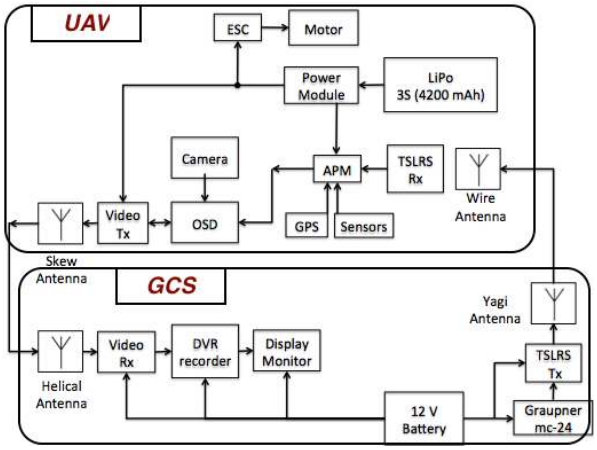

Figure 4: Block diagram showing the remote person view sub-system.

tised as having a 50 km range. The helical antenna will provide a 60 ° angle of beam width [11].

An on-screen display (MinimOSD) device is used to allow the telemetry module of the flight controller (APM) to overlay telemetry data onto the video stream which facilitates its navigation. This information includes primarily, airspeed, GPS coordinates, altitude, direction home, distance home, battery percentage, flight mode, travelled distance and RC signal strength cardinal orientation and aircraft roll, pitch and yaw.

The RPV camera is held in place by a gimbal which is able to isolate the movement of the airframe from the camera, keeping it levelled at all times. This is accomplished by using two servos for pan and tilt. Although the use of a camera gimbal through manual control shows great potential, the automonous stabiliser showed low capabilities due to the fact that the frame was covering most of the image when the UAV was climbing. This, of course, only disturbs the pilot. It is suggested that the autonomous tracking be used on a second camera gimbal (a second video system) whose purpose is not to pilot the UAV but to monitor the surrounding environment.

A block diagram of the entire RPV unit is presented in Fig. 3.

3.5. System Block Diagram

A simplified block diagram of the UAS is shown in Fig. 4. It shows the functional relationships between all the components that make up the UAS. Also, Figs. 5 show the UAS as it was used for the flight tests.

Regarding the strength of RF signals on the Scherrer (LRS) device, RSSI sensors on board of the UAV are able to measure that across a range of frequencies. The signals, although noisy and ambiguous due to structural noise, allow estimates to be made of emitter locations. The RSSI output is an analogue voltage that reveals how strong the signal arrives to the receiver. The range of the RC transmission is estimated with the antennas in line of sight, without any obstacles using the Friis transmission equation (Eq. 1).

$$\frac{P_r}{P_t} = G_t G_r (\frac{\lambda}{4\pi R})^2, \quad (1)$$

where P_r is the power available at the input of the receiving antenna; P_t is the output power to the transmitting antenna; G_t and G_r are the antenna gains with respect to the isotropic radiator of the transmitting and receiving antennas respectively, λ is wavelength and R the distance between the antennas. Table 1 provides the required data for estimating the range of the transmission.

Equation 1, retrieved from [12], is valid for propagation in free space without obstacles and it gives the value of the received power on the antenna.

Regarding the video system evaluation, the main limitation of today's theoretical approaches is that

(a) UAV.

(b) Ground station.

Figure 5: Final result for the UAS setup on the day of the first flight.

	Monopole	Yagi
Frequency [MHz]	433	433
Output Power [dBm]	26.99	26.99
Sensitivity [dBm]	-113	-113
Receiving Gain [dBi]	2	2
Transmitting Gain [dBi]	3	13
Fade Margin [dB]	20	20
Communications Range [km]	56	160

Table 1: RC link range with both Monopole and Yagi antennas.

they rely strictly on numeric comparison and do not actually take into account any level of biological factors of the human vision system [13, 14, 15]. In [16], it is provided some insights on why image quality assessment is so difficult by pointing out the weaknesses of the error sensitivity based framework.

Therefore, the chosen method of evaluation for this work is the subjective quality measurement, Mean Opinion Score (MOS) which consists on using the human eyes to simply evaluate the video quality in different situations using the following parameters of evaluation: colours, contrast, borders, movement continuity, flicker and smearing. In the whole UAS, the video sub-system is the most sensitive and so, the one that most suffers from disturbances. For this reason, they take part of the testing done to the video system in terms of propagation losses and also obstruction effects.

3.6. Weight and Propulsion

Before choosing a motor for the design, the total estimated weight of the UAV was determined and the required thrust and output power were estimated. This estimation is important because if the thrust provided by the motor is too little, the UAV will not respond well to control and will have difficulties performing manoeuvres. Also, if the motor is too strong it will be spending unnecessary energy.

Components	Weight (g)
Electric motor	102
Propeller	35
Camera	26
LiPo battery	349
Servos	132
Airframe	1000
ESC	80
RC Rx	16
Video Tx	21
OSD	5
GPS Rx	17
APM	30
Total Weight	1742 g

Table 2: List of components with their respective weight estimates.

The first assumption is that the climb stage is the one that requires more power and thrust. Also assuming that the climb stage will be at a constant rate, the required thrust for climbing can be estimated as [17]

$$T = W\sin(\gamma) + qSC_{D_0} + \frac{W^2}{q\pi AReS} \tag{2}$$

and also the required power is given by [17]:

$$P = T_{climb}V_{climb} \tag{3}$$

From [17] the required variables were estimated as shown in Table 3 where W refers to total weight, γ the climb angle, q the dynamic pressure, S the total wing area, C_{D_0} skin friction

This results in a required thrust of 8.11 N and a output power of 82.7 W. From the above estimate,

W (N)	20
γ (°)	20
q	61.25
S(m^2)	0.3944
C_{D_0}	0.022
AR	8.96
e	0.8
V_{climb} (m/s)	10

Table 3: Necessary parameters for calculating the required thrust and power.

an OS3810-1050 motor with a 10x5 propeller was chosen which gives the specifications as seen in Table 4 was chosen.

OS motor	3810-1050
Volts	12.6
kV(rpm/V)	1050
Weight (g)	102
ESC	50A
Battery	3S
Prop.	10"x5"
Max. Thrust (kg)	1.5
Max. Power (W)	328

Table 4: Main specifications of the OS3810-1050.

3.7. Battery Power

When choosing a battery, it is recommended that the amperage of the battery exceeds that of the motor. This ensures that even if the motor is running at 100 % the battery does not hold it back [18].

The motor's current is calculated as follows: Motor maximum power = 328 W
Battery voltage (LiPo 3S) = 11.1 V
Maximum motor current = 328/11.1 = 29.55 A.
A battery pack with discharge current rating above 29.55 A is therefore needed.

A three cell LiPo battery pack was chosen with the following specifications:
Battery capacity = 4.2 Ah.
Maximum discharge current = 45 C.
battery maximum discharge current = 4.2x45 = 189 A.
It is seen that the current of the battery well exceeds that of the motor and so it is suitable for the design.

The tests that were carried out on the prototype where divided into two major sections: controlled environment and flight testing.They would determine the level of conformation with the set objectives and are detailed in Sections 4 and 5.

4. Controlled Environment Tests

In this section, it will be addressed the multiple-fold problem of trading off in a set of mission requirements, balancing between the communications capabilities and the desired UAV radius of action. It is said that the system will be first evaluated in a controlled environment in the sense that it is being hold by a person two meters above the ground in seven discrete positions where there is no risk to the UAV or the surroundings.

4.1. Radio-Control Link System

The RSSI enabled the determination of the signal strength from one checkpoint to another, as seen in Fig. 6. A test to the radio-control link determined, 2 m above the ground, that using a directional (the Yagi) antenna will give double the range of an omnidirectional (whip) from 4 to 8 km. However, a new factor emerges: the antenna has to be manually oriented. Also, the use of more than 0.5 W as output power is only justified only at an 8 km distance. These estimates are very conservative due to the fact they are performed 2 m above the ground. In flight, at 1000 m altitude better results are expected.

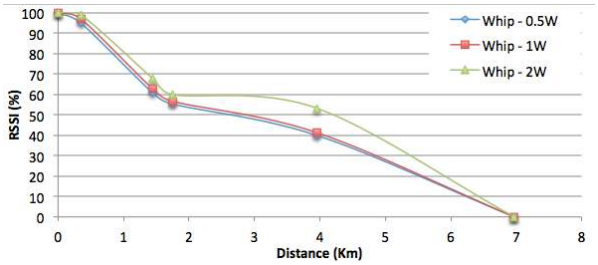

(a) RSSI versus distance home with Monopole antenna.

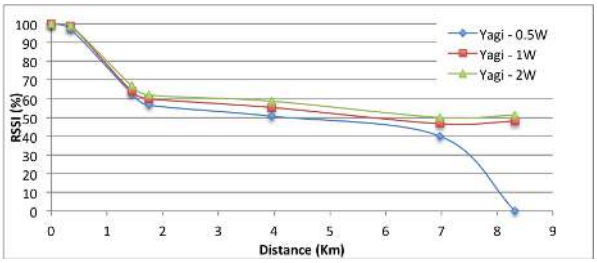

(b) RSSI versus distance home with Yagi antenna.

Figure 6: Changing the output power and antennas of the transmission.

4.2. Video Link System

A test to the video system was able to evaluate the quality and range of the signal with certain antenna configuration (exchanging between monopole and skew planar antennas on the UAV between monopole and helical antennas on the ground station) in terms of propagation loss, polarization loss, banking manoeuvres and response to obstruction. Since contrast, colours, borders movement continuity, flickering and smearing seemed to be equally affected by the distance, the video signal was clas-

sified by a generalized parameter, named overall image quality, seen in Fig. 7.

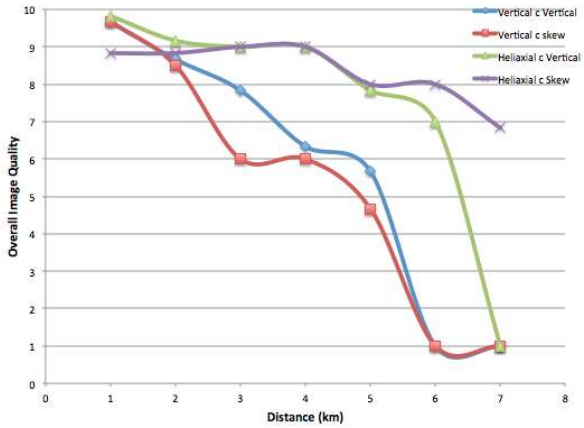

Figure 7: Video quality affected by propagation loss.

The best configuration for a long range flight is a circularized polarization one using a high gain antenna on the ground station which retrieved a maximum distance of 7 km, as seen in Fig. 7. The circular polarization will overcome banking and obstructions and the directional antenna will allow coverage of a much further flight. However, as stated for the RC sub-system testing, having a directional antenna will increase the risk of losing link suddenly because of the Helical antenna directivity. The obtained estimates are very conservative due to the fact that they were taken 2 m above the ground: in 1000 m latitude flight, much better results are expected.

4.3. Interaction between Video and Communication Systems

Next, the interference between the RC sub-system and the video link is evaluated. On one hand, the onboard video system emits strong RF signals in its primary frequency and also in other frequencies (there is usually noise from spurious emissions) which affects other onboard equipment such as RC receiver, GPS receiver, stabilization systems and servos. On the other hand, GCS wise, the same goes for the RC transmitter. Its third harmonic can affect the video link quality because they are is stand very near from one another

Ground station wise, using the same evaluation scheme as in the standalone video test, it is possible to draw several conclusions: although it was expected RC interferences in the video sub-system it was shown a different kind of interference: the video system gets affected by the panels overlaying method of the MinimOSD.

Figure 8 presents the format for the ground station, with the UAV was being turned on and off at the predefined locations along the coast for the testing in controlled environment and Fig. 9 shows the way the same tests were conducted.

Figure 8: UAV capturing the ground station.

Figure 9: Testing in controlled environment.

Onboard wise, two different tests were performed: interference of video Tx with the GPS and video Tx with the RC receiver. With the performed tests there seems to be no interference into the GPS receiver. Regarding the RC receiver, the values of the RSSI were retrieved for seven discrete checkpoints with the video system turned on and these results were compared with the ones retrieved from the RC standalone testing, as seen in Tables 5 and 6.

	Yagi	0,35km	1,5km	2km	4km	7km	8km
RSSI	0.5W	97	63	57	51	40	0
	1W	99	64	60	55	47	48
	2W	99	67	62	59	50	51

Table 5: Performance of the RC system with the Yagi configuration retrieved from the RC standalone testing.

The results retrieved from the UAV platform are outstandingly better than the ones retrieved from the RC standalone platform since the UAV, at 8

	Yagi	0.6 km	2 km	3 km	4 km	6 km	8 km
RSSI	0.5W	95	95	93	92	92	84
	1W	96	96	95	95	95	87
	2W	97	97	97	97	97	90

Table 6: Testing the performance of the communications system on the Yagi configuration while the RSSI is provided by the video link.

km is still showing a strong signal of 84%. This can only be due to the change in environment. The RC sub-system despite being digital (less prone to interference from the environment), can still be affected by the area where it is transmitting in.

5. Range Flight Tests

The flight tests were performed in a track specially designed for Remote Control flights so that the pilot affiliated with that track club could legally fly the UAV.

5.1. Short Range Flight Testing

The testing of the range of the UAS is done step by step meaning that before extending the range of the flight many short range flights were used to study the UAS link quality. One of those flights is analysed next. This flight was performed in 'Manual' flight mode and both ground station antennas (Yagi and Helical) were used and never moved during the whole flight test.

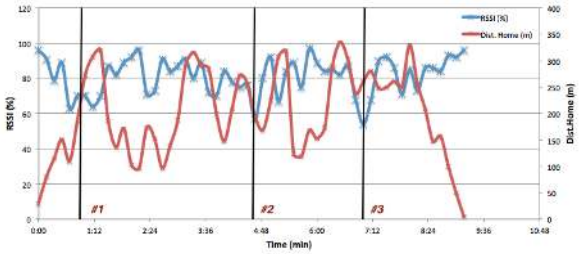

Figure 10: RSSI versus distance home.

Regarding RC link quality, Fig. 10 shows three distinct pinpoints and they all represent periods where the UAV went out of the Yagi's beam width (which is 30°). This figure shows that even in short ranges the orientation of the Yagi antenna can be crucial.

From Fig. 11, it is possible to analyse the influence of banking manoeuvres on the signal strength. The diversity feature of the RC LRS receiver is properly effective; minute 1:40 serves as an example: the UAV has a roll angle of -39° and the RSSI retrieves 85%.

Regarding video quality of the same short range flight, although the UAV never got out of the Helical antenna beam width there are still some video glitches provoked by undetermined interferences. The degradation of video quality due to the coding of the MinimOSD was noted mainly around the

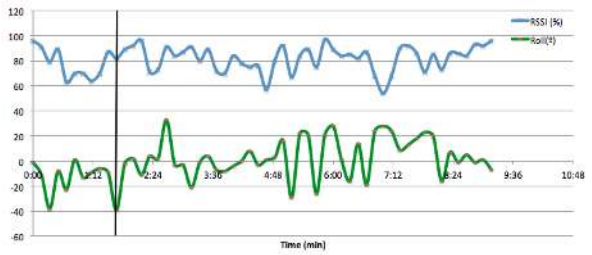

Figure 11: RSSI versus the roll of a certain manoeuvre.

telemetry data.

The maximum distance from home of the flight was 396 m with a travelled distance 4830 m and 65% left of battery percentage.

5.2. Long Range Flight Testing

This flight was also performed in 'Manual' flight mode and both ground station antennas (Yagi and Helical) were used and, for safety reasons, oriented towards the UAV so that the signal strength was as high as possible. Figure 12(b) shows the path taken for this flight test.

Regarding the RC link quality, the farther the UAV was, the more difficult it was to orient the Yagi and the sense of orientation of the pilot played a major role in the aspect. The relation between the distance home and the RSSI, it is seen from Fig. 13 that comparing with the ground test, from Fig. 13 ground effects greatly influence the link since, on the ground, at 2 km distance, the RSSI retrieved 60% and in the air (at 480 m of altitude) the RSSI retrieves 80%. The three drops in RSSI seen in the same Figure were always caused by the orientation of the Yagi antenna. Although the signal strength is influenced by propagation loss (distance home), the parameter that most affects this flight is the directivity of the antenna. Comparing the performance on the ground it can be said that this system can top a range of, at least, 7 km.

As done for the short range flight, this flight is also analysed in terms of video issues (and quality). The Helical antenna was hand-oriented so that risks video issues were minimized.

At this checkpoint, two situations are noteworthy: the polarization loss issue, seen in Fig. 14(a) and obstruction, in Fig. 14(b). At a 53° bank angle, there are no interferences so the circular polarization proved itself, once again, useful. As for the obstruction, one person stood right in front of the Helical antenna and the conclusions from ground testing were confirmed: although circular polarization appears to rectify the obstruction, it is still affected by it. As the UAV got higher, the video link got clearer. Reorientating the Helical antenna becomes an issue in kilometre 2 where the image starts

(a) UAV flying by the ground station.

(b) Flight path for the 2200m range test.

(c) Video capture of the UAV near the ground station.

Figure 12: Flight testing.

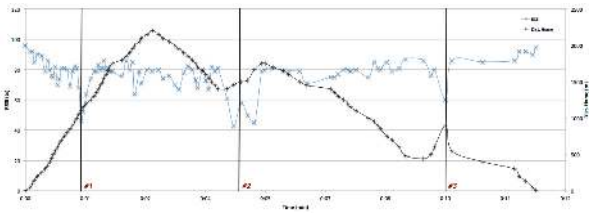

Figure 13: Overall flight data for a short range flight.

(a) UAS performing a banking manoeuver.

(b) Obstructed heliaxial antenna.

Figure 14: First pinpoint (#1) remarks.

flickering and smearing. Moving 100 m North improves the video link significantly as seen from Figs. 15. It is noteworthy to compare the colours from Figs. 12(c), near the ground station, 14(a), 10 m away and 15(b) as long as the camera is pointing to the sky the image turns grey but it stays like that dispite the distance: this is a camera issue and not transmission.

When the maximum flight range of 2193 m is achieved, the image starts to get smeared as previously and the pilot decides to return home since moving the antenna in the wrong direction could losing the video link completely which was an unnecessary hazard.This does not mean that the maximum range of the video link is actually 2 km, it just means that as the distance home grows it gets dangerous to reorient the antenna.

The risk of losing the video and/or RC links in the middle of a long range flight is a threatening reality. The use of antenna tracker is something to consider. However, this antenna tracker will required a long range transceiver system. A solution with the 3DR telemetry and a directional antenna could give the tracker more than the announced 1 km range but the output power of 100 mW really limits the applications of this approach.

(a) Video loss at 2.03 km from the GCS (#5).

(b) Image recover after reorienting Helical antenna.

Figure 15: Remarks from pinpoints #5 and #6.

6. Design of an Antenna Tracker

Antenna trackers are systems that track the UAVs location, and use this information to correctly align a direction antenna. From ground and flight testing it was found that in long distances it was hard to point the antenna to where the UAV was exactly and for this reason, the design of an antenna tracker is addressed in this appendix. This approach significantly improves the range over which signals can be both sent and received from the ground station.

The main problem of using the 3DR-transceiver is that the ground station would have three antennas with two of then working in the 433 MHz frequency band which is not advisable due to interference reasons.

Thus, a different solution was approached. The design is retrieved from a post of Alexander Greve in RCGroups [19] that designed an antenna tracker which, instead of using GPS coordinates to determine azimuth (heading) to direct the antennas beam, uses raw signal strength (RSSI). Using three similar directional antenna doing a 45° angle with one another as in the case of Fig. 16, it is possible to orient the middle antenna to the direction of the lateral antenna with the highest value of RSSI.

This design was chosen because this antenna tracker, working properly will have the same range as the video system (and not the range of the the telemetry system adaptation). Figure 16 shows Alexander Greve's own prototype.

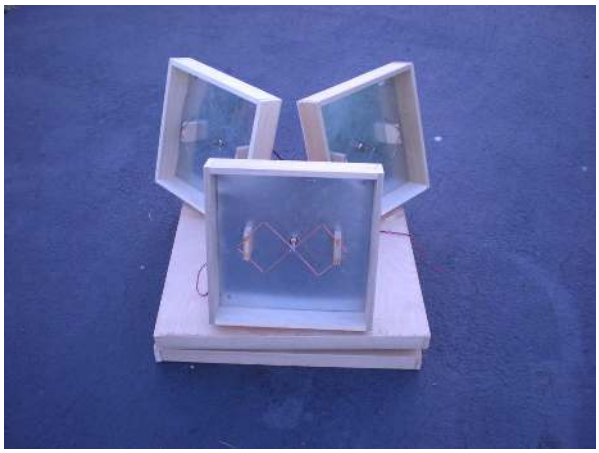

Figure 16: Alexander Greve's own prototype [19].

7. Conclusions

This work has been able to present the design and construction of a remote person view (RPV) with long range capabilities to be used for civilian applications in areas such as surveillance and information gathering. The long range mark of 100 km was not met since system urged for antenna tracking and instead a conservative estimate of 10 km mark was reached. Ground and flight tests uncovered issues and some have been corrected, polarization loss and obstruction serve as examples. However, a lot still needs to be done in terms of the correct use of directional and high gain antennas and also with regards to energy consumption. This prototype and respective performance are summarized in Fig. 17

References

[1] André C. Marta and Pedro V. Gamboa. Long endurance electric UAV for civilian surveillance missions. In *29th Congress of the International Council of the Aeronautical Sciences, St. Petersburg*, 2014.

[2] M. C. Quilter and V. J. Anderson. *Low altitude large scale aerial photographs: A tool for range and resource managers*. Society for Range Management, 1969.

[3] P.J. Hardin and M.W. Jackson. An unmanned aerial vehicle for rangeland photog-

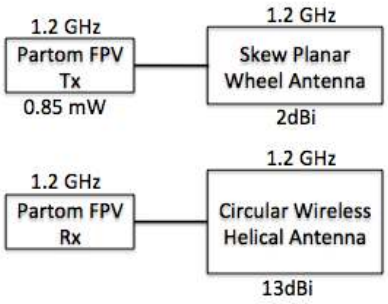

(a) RPV long range configuration.

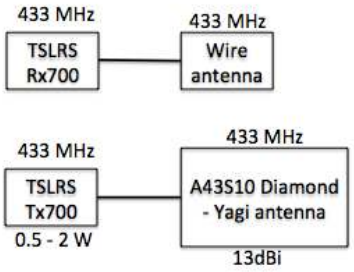

(b) RC long range configuration.

	Controlled Environment	Flight
RC	>8 km	>2 km
Video	8 km	>2 km

(c) Ranges in controlled environment and in flight tests.

Figure 17: Final configuration for long range flights.

raphy. *Rangeland Ecology and Management 58(4): 439-442*, 2005.

[4] V. Espinar and D. Wiese. An extreme makeover: scientists upgrade a toy plane with robotic technologies. *GPS World*, pages 20–27, 2005.

[5] Roberto Montiel. Record de alcance en aeromodelismo radiocontrolado mediante cámara subjetiva (fpv). https://vimeo.com/49417422. Accessed: 2015-05-10.

[6] D. L. Figueiredo. Autopilot and ground control station for uav. M.s. thesis, Instituto Superior Técnico, oct 2014.

[7] Scherrer UHF Long Range System. Manual for tx700. November 2013.

[8] Diamond Antenna. A430s10 base station Yagi beam datasheet. January 2007.

[9] ElectronicaRC. Partom 850 mw 1.2ghz video system datasheet. May 2014.

[10] Circular Wireless. Skew planar wheel datasheet. January 2007.

[11] Circular Wireless. Helical modo axial datasheet. January 2007.

[12] Carlos Fernandes. Estimar o alcance de uma ligação assumindo desimpedida utilizando a equação de friis. Portugal 2014.

[13] Q. Huynh-Thu and M. Ghanbari. Scope of validity of psnr in image/video quality assessment. *Electronics Letters*, 22(13), 2012.

[14] Yusra A. Al-Najjar and Dr. Der Chen Soong. Comparison of image quality assessment: Psnr, hvs, ssim, uiqi. *International Journal of Scientific and Engineering Research*, 3(8), 2012.

[15] National Instruments. Peak signal-to-noise ratio as an image quality metric. National Instruments, 2013.

[16] Zhou Wang. Why is image quality assessment so difficult. *Acoustics, Speech and Signal Processing (ICASSP)*, IV:3313 – 3316, 2002.

[17] T. C. Corke. *Design of Aircraft*. Pearson Education, 2003. ISBN 13: 978-0130892348.

[18] C. Ononiwug and O.J. Onojo et al. Uav design for security monitoring. *International Journal of Emerging Technology & Research.*, II(2), March 2015.

[19] Alexander Greve's Do It Yourself Antenna Tracker. http://www.rcgroups.com/ forums/showthread.php?t=1337608. Accessed: 2015-05-10.